Mechanistic Determination Using Arrays of Variable-Sized Channel Microband Electrodes: The Oxidation of Ascorbic Acid in Aqueous Solution

Francisco Prieto, Barry A. Coles, and Richard G. Compton*

Physical and Theoretical Chemistry Laboratory, Oxford University, South Parks Road, Oxford OX1 3QZ, U.K.

Received: May 1, 1998; In Final Form: June 30, 1998

"Two-dimensional voltammetry" using arrays of variable-sized gold channel microband electrodes in combination with variable flow rate measurements together with independent gold rotating disk electrode (RDE) data is applied to characterize the oxidation mechanism of L-ascorbic acid (AH_2) to dehydro-L-ascorbic acid in aqueous solutions. At pH 2.1 and very low mass transport conditions the reaction is consistent with a CECE mechanism, while at higher mass transport conditions an $EC_{fast}CE$ mechanism is followed. At pH 6.7, the results are again consistent with an ECE mechanism. The following mechanism is proposed: $AH_2 \rightleftharpoons AH^- + H^+$ (k_{CEE}), $AH^- \rightarrow AH^\bullet + e$, $AH^\bullet \rightarrow A^{\bullet -} + H^+$ (k_{ECE}), $A^{\bullet -} \rightarrow A + e$ (CECE); $AH_2 \rightleftharpoons AH_2^+ + e$, $AH_2^+ \rightarrow AH^\bullet + H^+$(fast), $AH^\bullet \rightarrow A^{\bullet -} + H^+$ (k_{ECE}), $A^{\bullet -} \rightarrow A + e$ ($EC_{fast}CE$); where, only the first pathway applies at pH 6.7, AH^- being the starting species. Values of 3.4×10^3 s^{-1} and 500 s^{-1} are found for the rate constants k_{CEE} and k_{ECE}, respectively.

1. Introduction

During the last three decades much effort has been made to elucidate the mechanism and the kinetics of the electrochemical oxidation of L-ascorbic acid[1−13] on different metallic electrodes. It has been established[10] that its first oxidation wave corresponds to the transfer of two electrons and two protons, forming dehydro-L-ascorbic acid, followed by the fast hydration of the latter species. Although a wide literature has been published on the subject, the full sequence of deprotonation and electron-transfer steps involved in the overall reaction is still not clear.

The most complete kinetic studies of the oxidation of L-ascorbic acid were performed by Aldaz et al.,[4−9] who demonstrated[4] the existence of a radical anion as an intermediate species in the two-electron oxidation of L-ascorbic acid at Pt, Ga, Au, and Hg electrodes, using the electron paramagnetic resonance (EPR) technique. This observation clearly indicated that the electron transfers proceeded in two separate steps. In further studies of Aldaz and co-workers the oxidation of L-ascorbic acid on Hg was studied[5−7] using polarography, and on Au,[8] using cyclic voltammetry. The results obtained led to the proposed mechanism for this reaction in acid and neutral mediums on both electrodes, given in Scheme 1. In this mechanism a predissociation was proposed as the first step, giving the monoanionic species. Then, a reversible one-electron, one-proton oxidation leads to the ascorbic acid radical anion that undergoes an irreversible one-electron oxidation to dehydro-L-ascorbic acid, which then undergoes a conventional hydration mechanism of a carbonyl group.[14] The time scale corresponding to the polarographic and voltammetric experiments used to propose the mechanism mentioned above did not permit the determination of the exact sequence of electron and proton transfers in the second step of Scheme 1.

The recently developed technique of 2-dimensional voltammetry uses an array of channel microband electrodes,[15] ranging in size from the millimeter to the submicron scale, and has been demonstrated to be a highly sensitive mechanistic and kinetic probe of diverse electrode processes which include coupled chemical steps. The use of both variable electrode size and convection implies that each electrode has its own characteristic kinetic window at a particular flow rate, so the joint combination of variable flow rate and electrode size provides an electrochemical kinetic tool capable of covering a wide range of rate constants, and in particular is very sensitive to the determination of reaction mechanism.

The aim of this paper is to seek further clarification of the mechanism of the oxidation of L-ascorbic acid, using the 2-dimensional voltammetry technique in combination with rotating disk electrode (RDE) experiments.

SCHEME 1

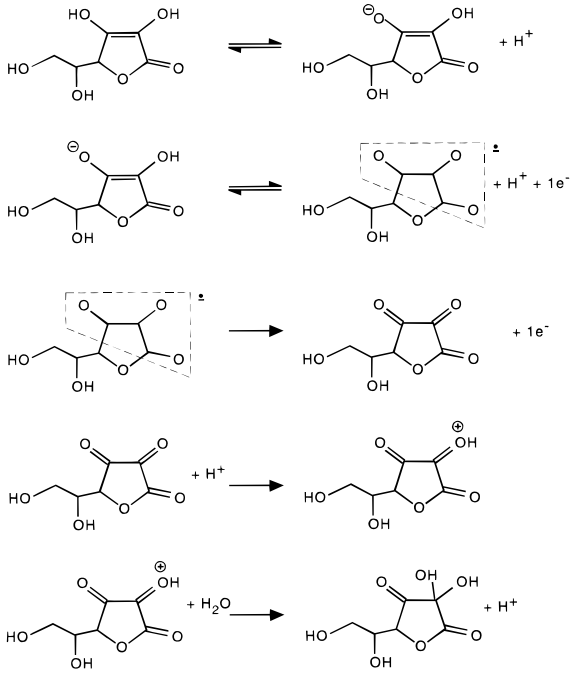

* Author to whom correspondence should be addressed.

S1089-5647(98)02080-X CCC: $15.00
Published on Web 08/25/1998

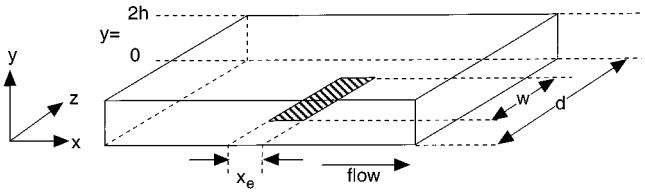

Figure 1. Schematic diagram of a channel electrode showing the geometric parameters and the coordinate system used to characterize the flow cell.

2. Theory

The 2-dimensional voltammetry experiments can be analyzed in terms of the independent responses of microband channel electrodes of different dimensions at various flow rates. A schematic diagram of a single microband channel electrode is given in Figure 1, where w is the width of the electrode and x_e is its length; $2h$ and d are the height and the width of the channel respectively; x is the coordinate in the flow direction and y is that normal to the electrode surface.

For an ECE mechanism:

$$\text{E step} \quad A \pm e^- \rightarrow B \tag{i}$$

$$\text{C step} \quad B \rightarrow C \tag{ii}$$

$$\text{E step} \quad C \pm e^- \rightarrow \text{products} \tag{iii}$$

where C produced in step ii is readily consumed in step iii, the steady-state mass balance equations are

$$0 = D_A\frac{\partial^2[A]}{\partial x^2} + D_A\frac{\partial^2[A]}{\partial y^2} - v_x\frac{\partial[A]}{\partial x} \tag{1}$$

$$0 = D_B\frac{\partial^2[B]}{\partial x^2} + D_B\frac{\partial^2[B]}{\partial y^2} - v_x\frac{\partial[B]}{\partial x} - k_{ECB}[B] \tag{2}$$

$$0 = D_C\frac{\partial^2[C]}{\partial x^2} + D_C\frac{\partial^2[C]}{\partial y^2} - v_x\frac{\partial[C]}{\partial x} + k_{ECB}[B] \tag{3}$$

where k_{ECE} is the rate constant of the homogeneous chemical step (ii) and v_x is the flow velocity in the x direction, which is a parabolic function of y:

$$v_x = v_0\left\{1 - \frac{(h-y)^2}{h^2}\right\} \tag{4}$$

with v_0 the velocity at the center of the channel

$$v_0 = \frac{3\,v_f}{4\,hd} \tag{5}$$

where v_f is the solution volume flow rate. Note that in writing eqs 1−3 we are assuming that the kinetic decay of B is irreversible.

Under conditions where the time taken to diffuse across the depth of the channel ($2h$) is long compared to the time taken to be transported along the length of the electrode, so that if

$$\frac{(2h)^2}{D_A} \gg \frac{x_e}{v_0} \tag{6}$$

the Lévêque approximation[16] applies, the parabolic velocity profile can be linearized at $y \sim 0$:

$$v_x = v_0\left\{1 - \frac{(h-y)^2}{h^2}\right\} = v_0\left(1 + \frac{h-y}{h}\right)\left(1 + \frac{h-y}{h}\right) \approx \frac{2v_0y}{h} \text{ for } y \approx 0 \tag{7}$$

The mass transport limiting current for an ECE mechanism is characterized by the effective number of electrons transferred, N_{eff}, which lies between 1 and 2.[17−19] Dimensional analysis shows that, if the Lévêque approximation holds and the diffusion coefficients for species A, B, and C can be considered equal ($D = D_A = D_B = D_C$), N_{eff} is a sole function of two dimensionless parameters.[20] These are the shear Peclet number:

$$P_s = \frac{3x_e^2v_f}{2h^2dD} \tag{8}$$

and a dimensionless rate constant:

$$K_{ECE} = \left\{\frac{k_{ECE}x_e^2}{D}\right\}\{P_s\}^{2/3} \tag{9}$$

Equations 1−3 can be solved numerically using the strongly implicit procedure[21,22] (SIP) or the multigrid method.[23] The results of these simulations can be stored in the form of "working surfaces" in which N_{eff} is tabulated as a function of P_s and K_{ECE}. The working surface provides a direct and readily accessible method to analyze the 2-D voltammetric steady-state response, by comparison of the experimental N_{eff} versus P_s and K_{ECE} surface with the theoretical one. The quality of the agreement between the experimental and theoretical surfaces is obtained through evaluation of the variance, defined as follows:

$$\text{variance} = \left(\frac{1}{n}\right)\sum_n\left(\frac{I_{lim(experimental)} - I_{lim(theory)}}{I_{lim(experimental)}}\right)^2 \tag{10}$$

where n is the number of experimental points within the boundaries of the simulated working surface.

The evaluation of the variance for different values of D and k_{ECE}, within ranges covering all conceivable cases, provides an error surface where the minimum yields the optimal values for the diffusion coefficient and the rate constant. This minimum search can be done automatically using the Golden Search Routine[24] or the Downhill Simplex algorithm.[25]

The consistency of any proposed mechanism, in this case an ECE mechanism, is checked using the optimal set of D and k_{ECE} values to generate the surface showing the ratio $I_{lim(experimental)}/I_{lim(theory)}$ versus log ($V_f/d/D$) and log (x_e/h). If the surface is featureless, notably if it does not show systematic deviations with the mass transport (which increases at higher V_f and/or lower x_e values), then the mechanism selected for the analysis is not inconsistent with the experimental results.

3. Experimental Section

The gold channel microband electrode array used is shown in Figure 2. The procedure followed to fabricate it has been described previously.[15] The array was mated with a channel unit made from optical grade fused synthetic quartz,[16] using low melting point wax. The mechanically measured dimensions of the channel were 0.5 cm width (d) and 0.035 cm height ($2h$). The channel including the microband array was incorporated into a conventional gravity-fed flow system capable of delivering volume flow rates in the range 10^{-4} to 5×10^{-1} cm^3 s^{-1}. The

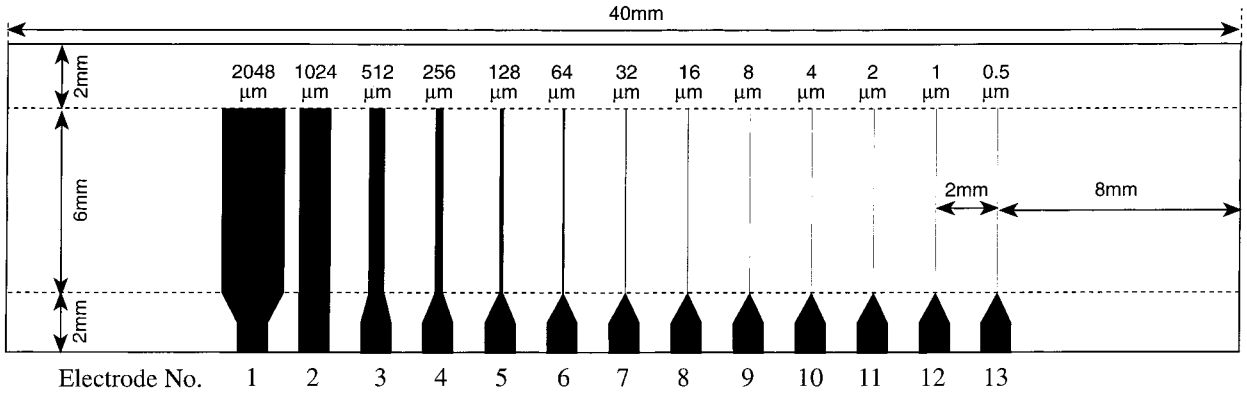

Figure 2. The channel electrode array.

channel was positioned with the longest electrode located downstream.

Voltammetric steady-state responses were obtained using a home-built three-electrode potentiostat controlled by an IBM-PC-compatible 486DX33 computer, running a Microsoft C^{2+} program. The potential scans were carried out for each of the 13 electrodes of the array automatically in turn, starting with the longest electrode, at a given flow rate. A saturated calomel electrode (SCE, Radiometer, Copenhagen) located upstream of the channel was used as reference electrode. The counter electrode was a platinum gauze mounted into a glass tube and positioned downstream of the cell to avoid possible contamination of the working electrode with counter-electrode electrolysis products.

The height of the assembled cell was calibrated using a solution of ferrocene in acetonitrile/0.1 M tetrabutylammonium perchlorate. Ferrocene undergoes a simple one-electron oxidation in this condition, and its diffusion coefficient is known.[27] The value obtained was 0.036 ± 0.001 cm, in close agreement with the value measured mechanically.

The rotating disk electrode (RDE) experiments were performed using an Oxford Electrodes rotator system capable of delivering rotation frequencies in the range 0.5−50 Hz. The working electrode used was a gold disk electrode with a diameter of 0.7 cm. The electrode was carefully polished using alumina suspensions of decreasing particle size up to 0.1 μm prior to each experiment. The electrochemical cell was completed employing the same reference and auxiliary electrodes as in the 2-D voltammetric experiments. Voltammetric RDE data were recorded using an Oxford potentiostat. Measurements were made at a temperature of 20 °C.

Aqueous solutions were made up using Elgastat (High Wycombe, Bucks, U.K.) UHQ grade water (18 MΩ cm). Solutions of ascorbic acid (99.7%, BDH, AnalaR) were prepared just before the experiment. All other chemicals were of analytical-reagent grade and used as received.

4. Results and Discussion

RDE Voltammetric Experiments. Steady-state voltammetry was conducted on solutions containing ca. 1 mM of L-ascorbic acid in aqueous phosphate buffer 0.2 M at pH 2.1 and 6.7 using a gold RDE at different rotation frequencies.

At pH 2.1 a steady-state voltammogram with an $E_{1/2}$ value of 0.26 V vs SCE was observed at lowest frequencies (ca. 1 Hz), in good agreement with the voltammetric results obtained by Rueda et al.[8] in the absence of convection. At higher rotation speeds a second wave appeared at more anodic potentials, as can be seen in Figure 3a for a rotation speed of 2 Hz. This second wave becomes larger compared to the first one when

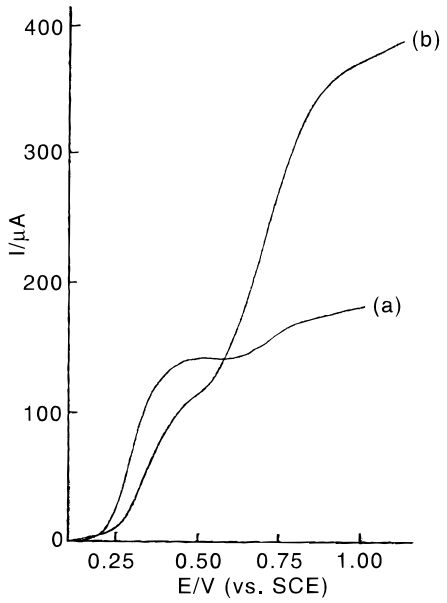

Figure 3. RDE voltammogram of a solution containing 1.008 mM of L-ascorbic acid in phosphate buffer 0.2 M (pH 2.1) at rotation frequencies of (a) 2.15 Hz and (b) 21.75 Hz.

the frequency increases, as is shown in Figure 3b, and both shift toward more positive potentials. At high frequencies the second wave completely overlaps the first one.

In Figure 4 is plotted the mass transport limiting current, I_{lim}, corresponding to the first wave and the sum of both waves as a function of the square root of the angular frequency of rotation. It can be seen as the I_{lim} values corresponding to the first wave do not follow the behavior predicted by the Levich equation[28] for a single-electron-transfer reaction:

$$I_{lim} = 0.620nFAD^{2/3}\nu^{-1/6}\omega^{1/2} \qquad (11)$$

with n being the number of electrons transferred, A the area of the electrode surface, ω the angular frequency of rotation in rad s^{-1}, and ν the kinematic viscosity in $cm^2\ s^{-1}$. From Figure 4 it can be seen that the effective number of electrons corresponding to the first wave decreases systematically with the rotation speed. On the other hand the total mass transport limiting current, including both waves, exhibits an excellent Levich behavior for a two-electron oxidation and from the slope of the linear plot a value of $(5.5 \pm 0.5) \times 10^{-6}$ $cm^2\ s^{-1}$ is obtained for the diffusion coefficient of L-ascorbic acid, in reasonable agreement with the value reported by Rueda et al.[8] of 6.7×10^{-6} $cm^2\ s^{-1}$.

A similar voltammetric behavior is found at pH 6.7, with the difference that the second wave overlaps the first one at

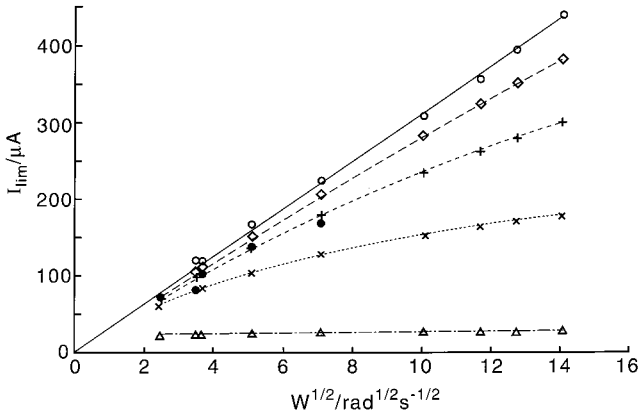

Figure 4. Mass transport limiting current as a function of $\omega^{1/2}$ for the same solution as in Figure 3: experimental values for the first wave (●), experimental values for the sum of first and second waves (○), generated values using eq 11 with $n = 2$ and $D = 5.5 \times 10^{-6}$ cm^2 s^{-1} (—), generated values using eq 12 with $n = 2$, $D = 5.5 \times 10^{-6}$ cm^2 s^{-1}, $K = 8.5 \times 10^{-3}$ and k_{CEE} values of 3.4 s^{-1} (—•—▽—•—), 3.4 × 10^2 s^{-1} (•••x•••), 3.4 × 10^{3}s^{-1} (— —+— —), and 3.4 × 10^4 s^{-1} (— —◇— —).

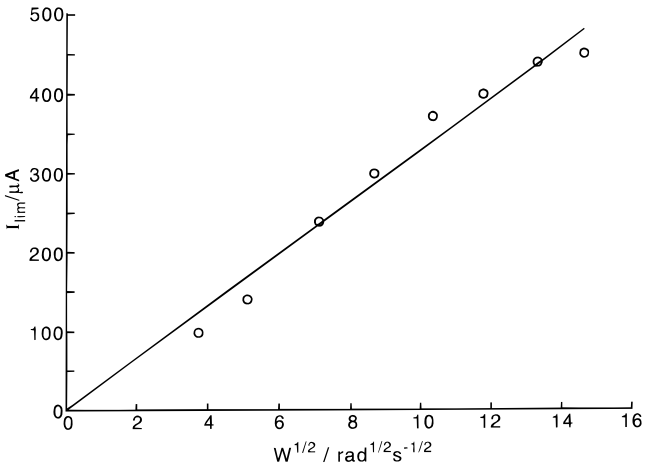

Figure 5. Mass transport limiting current as a function of $\omega^{1/2}$ for a solution containing 1.0 mM of L-ascorbic acid phosphate buffer 0.2 M (pH 6.7): experimental values for the sum of first and second waves (○), generated values using eq 11 with $n = 2$ and $D = 5.9 \times 10^{-6}$ cm^2 s^{-1} (—).

lower rotation frequencies and, therefore, it is not possible to obtain the mass transport limiting current for the first wave in a ω values range wide enough as to check the Levich plot. The total I_{lim} corresponding to both waves is represented in Figure 5 as a function of $\omega^{1/2}$, showing a linear behavior. A value of (5.9 ± 0.9) × 10^{-6} cm^2 s^{-1} for D is obtained from the slope assuming two electrons are passed in the oxidation.

The behavior observed at pH 2.1 can be understood on the basis of a parallel pathway mechanism in which the first wave corresponds to a reaction scheme with a preceding rate-determining chemical step followed by two successive electron-transfer steps, this is an CEE mechanism. As the rate mass transport increases, increasing the rotation speed, the N_{eff} value will decrease, deviating from the Levich behavior for a single-electron transfer. A second pathway becomes possible at higher overpotentials, which does not include the preceding chemical step. This second pathway corresponds to the second wave observed in the RDE voltammetric experiments, and the fact that the total I_{lim} follows a good Levich plot for a two-electron oxidation indicates that there is not any chemical step affecting the mass transport limiting current, either because all the possible

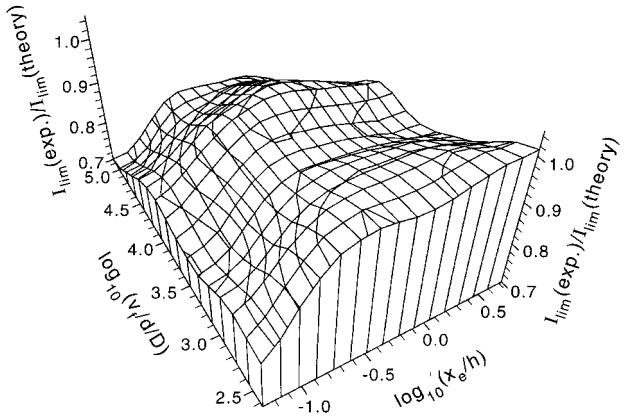

Figure 6. Surface showing $I_{lim(experiment)}/I_{lim(theory)}$ as a function of $\log(x_e/h)$ and $\log(v_f/d/D)$ for a solution containing 1 mM L-ascorbic acid in phosphate buffer 0.2 M at pH 2.1, analyzed according to an EE mechanism.

chemical steps are after the second electron-transfer step (an EEC mechanism) or because any chemical step preceding the second electron transfer is not rate determining within the time window of the RDE experiment (an ECE mechanism where the chemical step is fast). Obviously, an analysis based on the RDE I_{lim} does not permit us to distinguish between both possibilities, and a different experimental technique, capable of covering a wider range of kinetic parameters, is desired in order to clarify which reaction scheme corresponds to the second pathway. We return to this issue in the following subsection.

On the other hand, the deviation of the I_{lim} values corresponding to the first wave obtained at pH 2.1 from the Levich behavior can be used to obtain the chemical step rate constant (assuming a CEE mechanism). According to the mechanism proposed in the literature[5−8] and taking into account that values of pK_{a1} and pK_{a2} for L-ascorbic acid are 4.17 and 11.57, respectively,[29] so that the reactant species at pH 2.1 is the neutral L-ascorbic acid, it seems that the chemical step should be the first deprotonation of L-ascorbic, preceding the first electron transfer.

The solution of the RDE convective-diffusion equations corresponding to a CE mechanism, with the chemical step being reversible, is reported in the literature,[30] and the mass transport limiting current expression is:

$$I_{lim} = \frac{nFADc^*}{1.61D^{1/3}\omega^{-1/2}\nu^{1/6} + \dfrac{D^{1/2}}{Kk^{1/2}}} \qquad (12)$$

with c^* being the bulk concentration of electroactive species, K the equilibrium constant of the chemical step, and k the sum of the forward (k_{CEE}) and backward (k_{-CEE}) rate constants of the chemical step.

The data obtained at pH 2.1 have been analyzed according to eq 12. For K the ratio K_{a1}/a_{H^+} (8.5 × 10^{-3}) has been adopted, so the fit of the experimental I_{lim} versus $\omega^{1/2}$ for the first wave to eq 12 provides the value of $k = k_{CEE} + k_{-CEE}$, and from $K = k_{CEE}/k_{-CEE}$, the value of k_{CEE} is obtained from this analysis. In Figure 4 are plotted the theoretical curves of I_{lim} vs $\omega^{1/2}$ for different values of k_{CEE}. It can be seen as the theoretical plot with $k_{CEE} = 3.4 \times 10^3$ s^{-1} provides an excellent agreement with the experimental data.

Two-Dimensional Voltammetry. The steady-state voltammetric waves of solutions containing ca. 1 mM of ascorbic acid in the same buffer as the RDE experiments were studied at different flow rates using the array of gold channel electrodes.

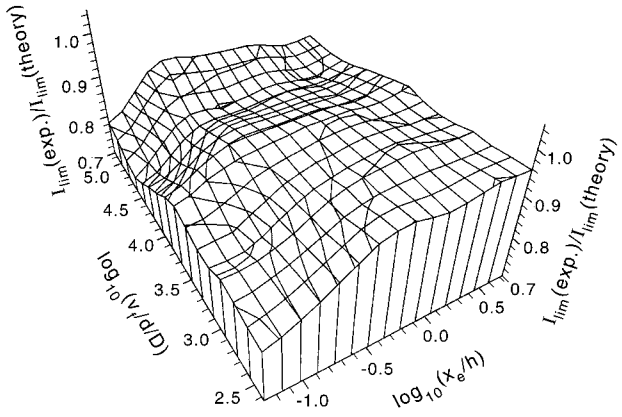

Figure 7. Surface showing $I_{lim(experiment)}/I_{lim(theory)}$ as a function of $\log(x_e/h)$ and $\log(v_f d/D)$ for a solution containing 1 mM L-ascorbic acid in phosphate buffer 0.2 M at pH 6.7, analyzed according to an EE mechanism.

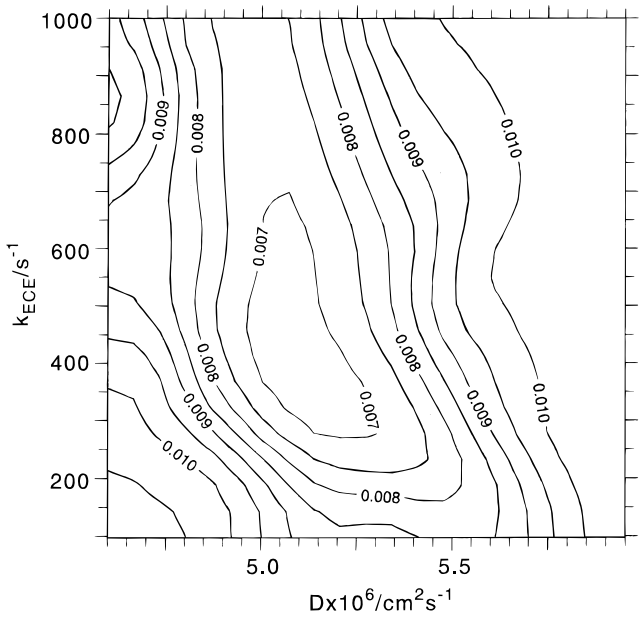

Figure 8. Surface showing the minimum variance corresponding to optmized D and k_{ECE} for a solution containing 1 mM L-ascorbic acid in phosphate buffer 0.2 M at pH 2.1, analyzed according to an ECE mechanism.

The $E_{1/2}$ values obtained at pH 2.1 and pH 6.7 were close to 0.750 and 0.300 V vs SCE, respectively, at lower mass transport conditions, corresponding to lower flow rates and longer electrodes.

The mass transport limiting currents obtained for different flow rates and electrodes were analyzed according to an EE mechanism following the procedure described in Theory. The ratio $I_{lim(experiment)}/I_{lim(theory)}$ is plotted as a function of $\log(x_e/h)$ and $\log(v_f d/D)$ in Figures 6 and 7 for pH 2.1 and 6.7, respectively. The values of D used were the same obtained from the RDE experiments. A clear trend can be observed on both plots: the ratio $I_{lim(experiment)}/I_{lim(theory)}$ systematically decreases with the mass transport, indicating the existence of a kinetic control of the limiting current.

These results also permit us to discard the EEC mechanism as the reaction scheme for the second pathway in the oxidation of L-ascorbic acid. An ECE mechanism was, therefore, adopted and the experiments analyzed according to it, with the diffusion coefficient and the chemical step rate constant as optimizable parameters. The surface showing the variance as a function of D and k_{ECE} gave a clear minimum corresponding to the optimum

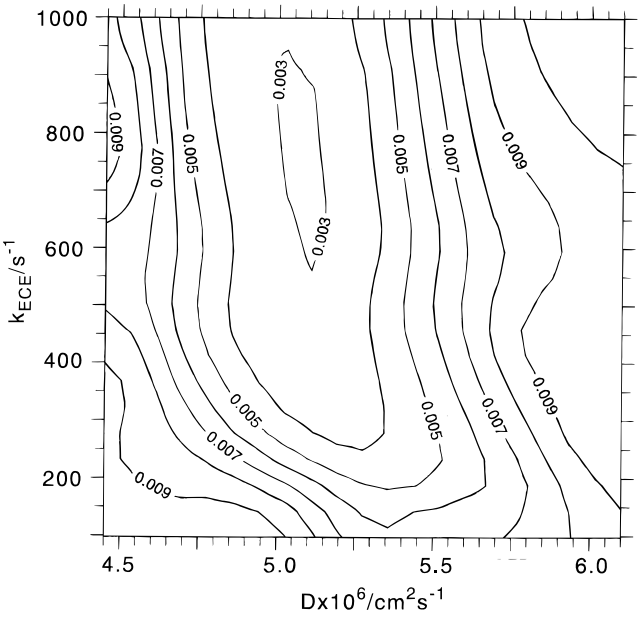

Figure 9. Surface showing the minimum variance corresponding to optmized D and k_{ECE} for a solution containing 1 mM L-ascorbic acid in phosphate buffer 0.2 M at pH 6.7, analyzed according to an ECE mechanism.

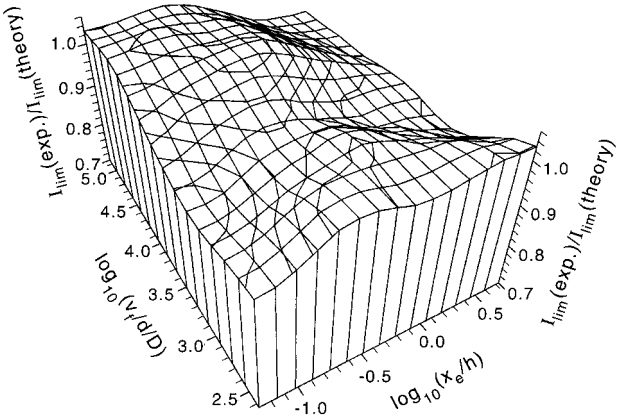

Figure 10. Surface showing $I_{lim(experiment)}/I_{lim(theory)}$ as a function of $\log(x_e/h)$ and $\log(v_f d/D)$ for a solution containing 1 mM L-ascorbic acid in phosphate buffer 0.2 M at pH 2.1, analyzed according to an ECE mechanism.

values of the adjustable parameters, as can be seen in Figures 8 and 9 for the experiments at pH 2.1 and 6.7, respectively. The relevant values are $D = 5.2 \times 10^{-6}$ cm^2 s^{-1} and $k_{ECE} = 335$ s^{-1} at pH 2.1 and $D = 5.1 \times 10^{-6}$ cm^2 s^{-1} and $k_{ECE} = 667$ s^{-1} at pH 6.7. In Figures 10 and 11 the surfaces of $I_{lim(experiment)}/I_{lim(theory)}$ versus $\log(x_e/h)$ and $\log(v_f d/D)$, obtained with these values of diffusion coefficient and rate constant are given. It can be observed that there is no systematic trend; the surfaces are essentially featureless and, therefore, the steady-state 2-D voltammetric experiments of L-ascorbic acid are consistent with an ECE mechanism, where the value for the rate constant of the chemical step is ca. 500 s^{-1}.

The agreement between the rate constants obtained at both pH 2.1 and 6.7 clearly suggests that the rate-determining chemical step is the same at both pH values and, therefore, it must correspond to the deprotonation of the radical formed after the first electron transfer and first deprotonation. Otherwise, different kinetics parameters should have been obtained for the very different pH values.

All these observations can be explained according to the

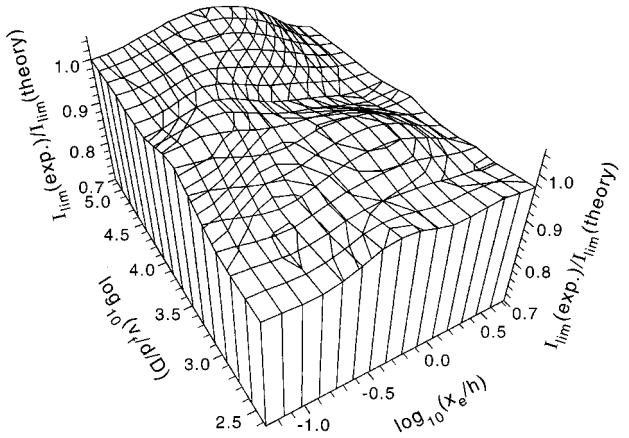

Figure 11. Surface showing $I_{lim(experiment)}/I_{lim(theory)}$ as a function of $\log(x_e/h)$ and $\log(v_t/d/D)$ for a solution containing 1 mM L-ascorbic acid in phosphate buffer 0.2 M at pH 6.7, analyzed according to an ECE mechanism.

SCHEME 2

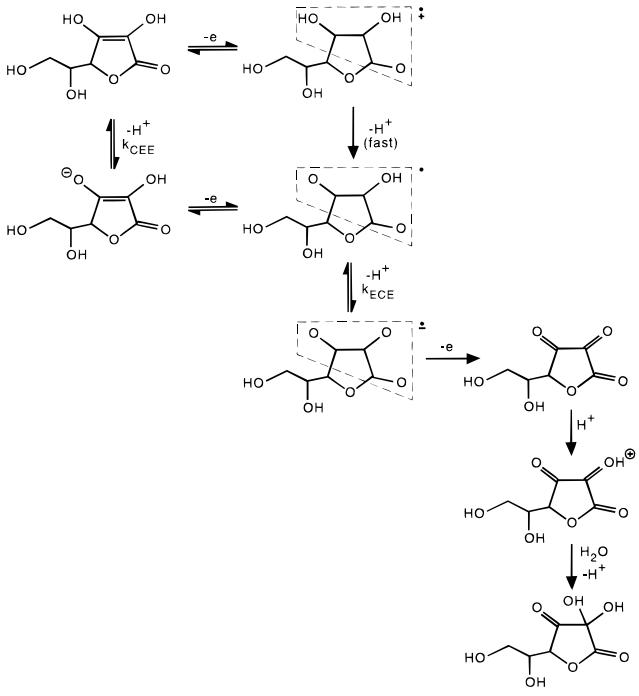

mechanism given in Scheme 2, where in the horizontal direction are represented electron-transfer steps and in the vertical one chemical steps. Note that the latter are either designated as preequilibria or as irreversible steps. The reaction scheme starts with L-ascorbic acid which can undergo either deprotonation to the monoanion followed by the first electron-transfer step to the radical which undergoes a second deprotonation to the radical anion (a CEC sequence), or the first electron transfer followed by a fast deprotonation and the rate-determining second deprotonation to the same radical anion (an $EC_{fast}C$ sequence). Then, the radical anion undergoes the second electron transfer to dehydro-L-ascorbic acid which follows the conventional proton-catalyzed mechanism of hydration of carbonyl groups.[14]

At pH 6.7, higher than pK_{a1}, the reaction starts with the ascorbic acid monoanion which undergoes an ECE sequence.

5. Conclusions

"Two-dimensional voltammetry" using channel electrodes in combination with RDE voltammetry has been applied to elucidate the mechanism of the oxidation of L-ascorbic acid to dehydro-L-ascorbic acid on gold electrodes. It has been proved that a parallel pathway mechanism is consistent with the experimental data: a CEC sequence in parallel to an $EC_{fast}C$ sequence and followed by a second E step, and the values of 3.4×10^3 s^{-1} and 500 s^{-1} have been obtained for k_{CEE} and k_{ECE}, respectively.

Acknowledgment. We thank the EC for financial support for F.P. (Grant No. ERBFMBICT950219).

References and Notes

(1) Brezina, M.; Koryta, J.; Loučka, T.; Maršiková, D. *J. Electroanal. Chem.* **1972**, *40*, 13.
(2) Koryta, J.; Pradáč, J.; Pradáčová, J.; Ossendorfová, N. *Experientia, Suppl.* **1971**, *18*, 367.
(3) Pradáč, J.; Pradáčová, J.; Koryta, J.; Vrubel, J. *Folia Biol. (Prague)* **1971**, *17*, 322.
(4) Aldaz, A.; Alquie, A. M. *J. Electroanal. Chem.* **1973**, *47*, 532.
(5) Dominguez, M.; Aldaz, A.; Sanchez-Burgos, F. *J. Electroanal. Chem.* **1976**, *68*, 345.
(6) Ruiz, J. J.; Aldaz, A.; Dominguez, M. *Can. J. Chem.* **1977**, *55*, 2799.
(7) Ruiz, J. J.; Aldaz, A.; Dominguez, M. *Can. J. Chem.* **1978**, *56*, 1533.
(8) Rueda, M.; Aldaz, A.; Sanchez-Burgos, F. *Electrochim. Acta* **1978**, *23*, 419.
(9) Acerete, C.; Garrigos, L.; Guilleme, J.; Diez, E.; Aldaz, A. *Electrochim. Acta* **1981**, *26*, 1041.
(10) Dryhurst, G.; Kadish, K. M.; Scheller, F.; Rennenberg, R. *Biological Electrochemistry*; Academic Press: New York, 1982; Vol. 1, p 256 (and references therein).
(11) Karabinas, P.; Jannakoudakis, D. *J. Electroanal. Chem.* **1984**, *160*, 159.
(12) Deakin, M. R.; Kovach, P. M.; Stutts, K. J.; Wightman, R. M. *Anal. Chem.* **1986**, *58*, 1474.
(13) Hu, I.; Kuwana, T. *Anal. Chem.* **1986**, *58*, 3235.
(14) Ingold, C. K. *Structure and Mechanism in Organic Chemistry*, 2nd ed.; Cornell University Press: Ithaca, New York, 1969; p 1014.
(15) Alden, J. A.; Feldman, M. A.; Hill, E.; Prieto, F.; Oyama, M.; Coles, B. A.; Compton, R. G.; Dobson, P. J.; Leigh, P. J. *Anal. Chem.*, **1998**, *70*, 1707.
(16) Lévêque, M. *Ann. Mines Mem. Ser.* **1928**, *12/13*, 201.
(17) Amatore, C.; Savéant, J. M. *J. Electroanal. Chem.* **1977**, *85*, 27.
(18) Amatore, C.; Gareil, M.; Savéant, J. M. *J. Electroanal. Chem.* **1983**, *147*, 1.
(19) Leslie, W. M.; Alden, J. A.; Compton, R. G.; Silk, T. *J. Phys. Chem.* **1996**, *100*, 14130.
(20) Alden, J. A.; Compton, R. G. *J. Phys. Chem. B* **1997**, *101*, 9741.
(21) Compton, R. G.; Dryfe, R. A. W.; Wellington, R. G.; Hirst, J. *J. Electroanal. Chem.* **1995**, *383*, 13.
(22) Stone, H. J. *SIAM J. Numer. Anal.* **1968**, *5*, 530.
(23) Alden, J. A.; Compton, R. G. *J. Electroanal. Chem.* **1996**, *415*, 1.
(24) Press, W. H.; Teukolsky, S. A.; Vetterling, W. T.; Flannery, B. P. *Numerical Recipes in C*, 2nd ed.; CUP: Cambridge, 1992.
(25) Nedler, J. A.; Mead, R. *Comput. J.* **1965**, *7*, 308.
(26) Coles, B. A.; Compton, R. G. *J. Electroanal. Chem.* **1983**, *147*, 1.
(27) Sharp, P. *Electrochim. Acta* **1983**, *28*, 301.
(28) Levich, V. G. *Physicochemical Hydrodynamics*; Prentice-Hall: Englewood Cliffs, NJ, 1962.
(29) *Merck Index*, 11th ed.; Merck: Rahway, NJ, 1989; p 858.
(30) Koutecky, J.; Levich, V. G. *Zh. Fiz. Khim.* **1958**, *32*, 1565; *Dokl. Akad. Nauk SSSR* **1957**, *117*, 441.